JOURNAL OF MATERIALS SCIENCE 26 (1991) 4561–4566

Phase transformation and microstructure in (Mg,Ti)-PSZ

W. S. LEE, A. C. SU, P. SHEN
Institute of Materials Science and Engineering, National Sun Yat-Sen University, Kaohsiung, Taiwan

Phase transformation and microstructure in Mg-PSZ (8 mol% MgO), sintered (1600 °C, 6 h) with 0 to 15 mol% additions of TiO_2 (designated as 0T to 15T specimens), were studied by X-ray diffraction and electron microscopy. According to the room-temperature X-ray lattice parameter, the saturation of TiO_2 in the cubic (c-) zirconia was reached at a total TiO_2 addition of ca. 6 mol% at 1600 °C, whereas the solubility limit in tetragonal (t-) zirconia was not reached in the composition range studied. The amount of t-zirconia increases with increasing TiO_2 content at 1600 °C, as indicated by the monoclinic (m-) zirconia content in the furnace-cooled specimens. Regardless of the modification of the lattice misfit strain by TiO_2 dissolution, the precipitates of t-phase in the c-matrix remain lenticular with {1 0 0} habit plane. Loops, due probably to condensation of the structural vacancies, were found in the m-phase of 9T, but not in 1T and 6T specimens.

1. Introduction

The morphology of tetragonal (t-) ZrO_2 in binary partially stabilized zirconia (PSZ) has been extensively studied [1–6]. In PSZ stabilized by MgO (Mg-PSZ) the t-ZrO_2 has a lenticular shape with a {1 0 0} habit plane (indexed according to the fluorite structure of c-ZrO_2) [1]. In PSZ stabilized by TiO (Ti-PSZ) the t-ZrO_2 also has a lenticular shape with a {1 0 0} habit plane [2]. In PSZ stabilized by CaO (Ca-PSZ) the t-ZrO_2 is equiaxed with a {1 0 1} habit plane [3]. In the early stage of precipitation in PSZ stabilized by Y_2O_3 (Y-PSZ) the t-ZrO_2 also has a {1 0 1} habit plane, but it commonly develops "colonies" of twin-related variants which do not readily transform to monoclinic (m-) ZrO_2 even when they become quite large [4]. Morphology features of t-ZrO_2 in ternary systems of (Mg,Ca)-PSZ [5], (Mg,Y)-PSZ [6] and in Y-PSZ/Ni_2AlTi cermet [7] have also been reported. Differences in the morphology and habit plane behaviour of the t-ZrO_2 phase in these systems have been attributed to the misfit in lattice parameters and interfacial energy between the t-ZrO_2 particles and the cubic (c-) matrix (c-ZrO_2) [6–8], following Khachaturyan's theory [9].

Phase assemblages of fired ceramics (1200–1750 °C) of the ZrO_2–MgO–TiO_2 ternary system have been studied by means of X-ray diffraction, optical microscopy and dielectric property measurements [10]. According to Coughanour *et al.* [10] addition of TiO_2 reduces the stability of the c-phase in Mg-PSZ. This ternary system has also been studied by Bateman *et al.* [11] using ZrO_2–MgO–TiO_2 powders prepared by a chemical route. Retention of the t-phase upon the addition of TiO_2 was observed. Detailed microstructural features, however, were not given by these authors. Reported here are results of our observations for (Ti,Mg)-PSZ sintered at 1600 °C using transmission electron microscopy (TEM), X-ray diffraction, and Fourier-transform infrared spectroscopy (FTIR).

2. Experimental procedure

The Mg-PSZ powder (8 mol% MgO, Toyo Soda, Japan) with 0 to 15 mol% (in 1% increments, designated as 0T, 1T, . . . , 15T, respectively) additions of TiO_2 (Merck, 99.9% pure) were ball-milled (6 h), dry pressed (40 MPa), then sintered (1600 °C, 6 h) and cooled in an open air furnace. It took more than 6 h for cooling from 1600 °C to below 400 °C. A $ZrTiO_4$ pellet for an FTIR standard was reactive-sintered (1550 °C, 44 h) from a stoichiometric mixture (ball-milled and dry-pressed as above) of ZrO_2 (Toyo, Soda, Japan) and TiO_2 (Merck, 99.9% pure) powders.

The surfaces of sintered specimens (polished with diamond paste, 1 μm in size) were analysed by X-ray diffractometry (CuK_α, 35 kV, 25 mA) for phase identification. The {1 1 1} diffraction peaks were used to estimate qualitatively the amount of m-ZrO_2 phase relative to the c- and t-ZrO_2 phases, the zirconia phases being indexed as a slightly distorted version of the c-fluorite unit cell. The identification of the c- and t-ZrO_2 phases in the {4 0 0} region of ZrO_2 was carried out with a step-scanning method (step size 0.02°, fixed count time 90 s, divergence and scatter slits 1°, receiving slit 0.2 mm). The lattice mismatch between c- and t-ZrO_2 was then estimated from the *d*-spacings of the {4 0 0} peaks.

The polished specimens were HF-etched at room temperature for 3–4 min and gold-coated for scanning electron microscopy (SEM), using the Jeol JSM-35CF instrument operating at 25 kV. The back-scattered electron image (BEI) and energy-dispersive X-ray

0022–2461/91 $03.00 + .12

(EDX) analysis were used to study the distribution of the alloying elements in the sintered specimens. Thin sections ca. 100 μm in thickness and 1 cm in diameter were microtomed from sintered pellets and dried in a dessicator for 3 days. Infrared spectra of these thin disks were then obtained by use of a Digilab FTS-40 Fourier-transform infrared spectrometer in transmission mode by coaddition of 256 scans in the spectral range of 800 to 300 cm^{-1} at 4 cm^{-1} resolution. Thin foils were prepared from dimple-ground thin sections (about 10 μm in thickness) by ion-milling and studied by TEM (Jeol 200CX at 200 kV).

3. Results

3.1. X-ray diffraction

For specimens containing less than 6 mol % TiO_2, the {400} *d*-spacing of the c-phase decreases as the TiO_2 content increases (Fig. 1). This is attributed to the substitution of smaller Ti^{4+} for Zr^{4+} and Mg^{2+}. The ionic radii of Ti^{4+}, Zr^{4+} and Mg^{2+} are 0.074, 0.084 and 0.089 nm, respectively, according to Shannon [12], if the coordination number is assumed to be 8. A constant X-ray lattice parameter is obtained for specimens containing more than 6 mol % additions of TiO_2, indicating that the solubility limit of TiO_2 in the c-phase is reached at a total addition of ca. 6 mol %. In contrast, the t-phase is not saturated with TiO_2 up to 15 mol % addition as indicated by the continuous decrease of the {400} *d*-spacing (and hence the lattice parameter along the *a*-axis, i.e. a_t) of the t-phase with increasing TiO_2 content (Fig. 2). The lattice parameter along the c-axis, designated as c_t, and the tetragonality (c_t/a_t) of the t-phase increase as the TiO_2 content increases (Table I). Note that the lattice misfit strain ε_{11} (along a_t) and ε_{33} (along c_t) increases with TiO_2 content (Table I). According to the ratio of {111} counts (Fig. 3), the increase in the quantity of m-phase is only slight as the TiO_2 content increases from 1 to 6 mol %. However, as TiO_2 content exceeds 6 mol %, the quantity of m-phase increases rapidly. For specimens of higher TiO_2 contents, our X-ray results indicate the presence of another phase which appears to be $ZrTiO_4$.

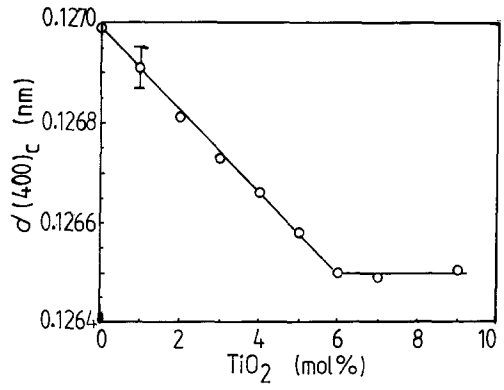

Figure 1 X-ray {400} *d*-spacing of c-phase in (Mg,Ti)-PSZ sintered at 1600 °C for 6 h.

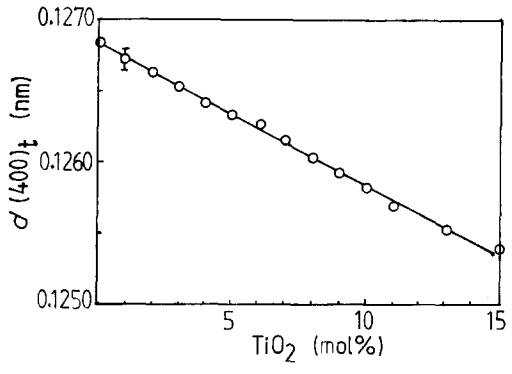

Figure 2 X-ray {400} *d*-spacing of t-phase in (Mg,Ti)-PSZ sintered at 1600 °C for 6 h.

3.2. FTIR spectra

In previous infrared spectroscopic studies of zirconia [13, 14], overlapping peaks (at least four for t-ZrO_2 and as many as nine for m-ZrO_2) have been identified in the spectral range of 800 to 200 cm^{-1}. In the case of c-ZrO_2, the absorptions are even more strongly overlapped, resulting in a broad band centred around 500 cm^{-1}. Among these absorptions, the one appearing in the 740 to 770 cm^{-1} range is relatively free of interference from other absorptions and is characteristic of m-ZrO_2. As shown in Fig. 4, FTIR spectra of (Mg,Ti)-PSZ are complicated by overlapping absorptions of various phases. However, the characteristic absorption band of the m-phase near 760 cm^{-1} [13, 14] is clearly discernible. The relative height of this peak increases with the TiO_2 content, especially when the latter exceeds 6 mol %. Another important feature in Fig. 4 is the gradual appearance of a shoulder at 550 cm^{-1} when the TiO_2 content exceeds 6 mol %. This is attributed to the presence of $ZrTiO_4$ which absorbs characteristically at this frequency. The absorption spectrum of $ZrTiO_4$ prepared by reactive sintering from a stoichiometric mixture of ZrO_2 and TiO_2 powders is given in Fig. 4g, where absorptions near 400, 450, 550 and 780 cm^{-1} are observable. Due probably to the limited amount of $ZrTiO_4$ and the overlap with absorptions of other phases, absorptions other than the 550 cm^{-1} peak are not as clearly identifiable. These observations are all consistent with the X-ray diffraction results above.

3.3. SEM observations

Our BEI and EDX results indicate the presence of a Ti-rich grain boundary phase in specimens with a TiO_2 content exceeding 6 mol %. This Ti-rich phase was identified as the $ZrTiO_4$ phase detected in our X-ray diffraction and FTIR studies. With or without the presence of $ZrTiO_4$, the sintered specimens with varied additions of TiO_2 always display distinct angles at the grain junctions (Fig. 5). Note that the free surface of the as-sintered specimens shows m-precipitates (Fig. 5a). This could be due in part to the grain-boundary and free-surface precipitation of m-ZrO_2. Fig. 5b shows a representative etched surface of sintered (Mg,Ti)-PSZ. Individual t-precipitate in the grain cannot be clearly resolved on SEM photographs of etched specimens (Fig. 5b), although its presence was confirmed by TEM observations described in the

TABLE I Room-temperature lattice parameters and habit planes for partially stabilized zirconia

	Mg-PSZ*	(Mg, Ti)-PSZ†		
		1T	6T	9T
a_c (nm)	0.5080	0.5080	0.5057	0.5057
a_t (nm)	0.5077	0.5073	0.5050	0.5037
c_t (nm)	0.5183	0.5188	0.5207	0.5217
c_t/a_t	1.021	1.023	1.031	1.036
ε_{11}‡	0.0006	0.0014	0.0014	0.0040
ε_{33}‡	0.0203	0.0213	0.0297	0.0316
$(a_t-a_c)/(c_t-a_c)$	− 0.029	− 0.065	− 0.047	− 0.125
Habit plane observed	{100}	{100}	{100}	{100}

* Taken from [6] and [8].
† Present work, Mg-PSZ (8 mol % MgO) with 1, 6 and 9 mol % TiO_2 for 1T, 6T and 9T specimens, respectively, sintered at 1600 °C for 6 h.
‡ $\varepsilon_{11} = \varepsilon_{22} = |(a_t-a_c)/a_c|$; $\varepsilon_{33} = |(c_t-a_c)/a_c|$.

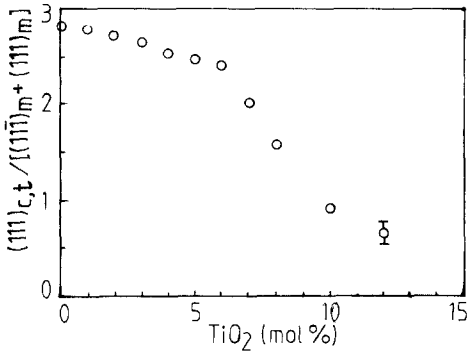

Figure 3 {1 1 1} zirconia counts ratio diffracted from polished (Mg,Ti)-PSZ sintered at 1600 °C for 6 h.

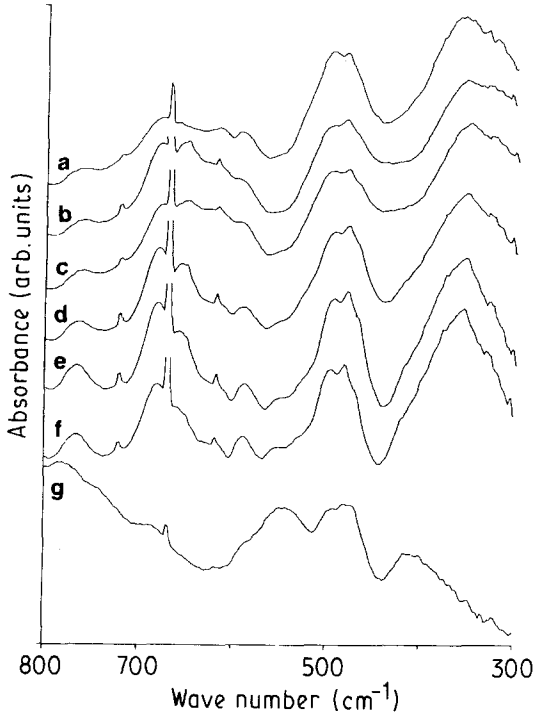

Figure 4 Representative FTIR spectra of (Mg,Ti)-PSZ specimens: (a) 0T (Mg-PSZ), (b) 3T, (c) 6T, (d) 7T, (e) 9T, (f) 15T, and (g) $ZrTiO_4$ standard prepared from constituent oxides. The sharp peak near 670 cm^{-1} is the artefact from atmospheric CO_2.

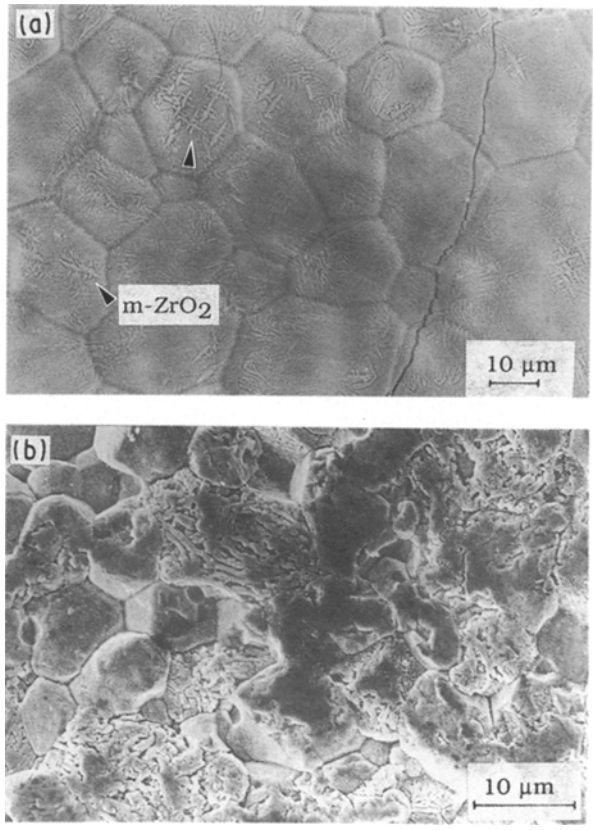

Figure 5 Representative secondary electron image of (Mg,Ti)-PSZ specimens: (a) as-sintered, 5T; (b) HF-etched at room temperature for 4 min, 12T specimen.

next paragraph. In general, the grain size of zirconia and the size of the t-precipitates within the grain increase with increasing TiO_2 content. However, the grain growth rate was suppressed in specimens with more than 6 mol % addition of TiO_2. This could be due to the presence of the additional $ZrTiO_4$ phase.

3.4. TEM observations

Three variants of the t-ZrO_2 phase were found in [$\bar{1}$ 1 1] selected-area diffraction (SAD) patterns of twinned zirconia grains of (Mg,Ti)-PSZ specimens (Fig. 6a), as in the binary PSZ system. Regardless of the amount of TiO_2 addition (Fig. 6b and c), diffuse scatter intensity (DSI) was commonly diffracted from the c-matrix, especially when the t-variants were out of contrast. The size of precipitates within the c-matrix (Mg,Ti)-PSZ specimens increased with the increase of

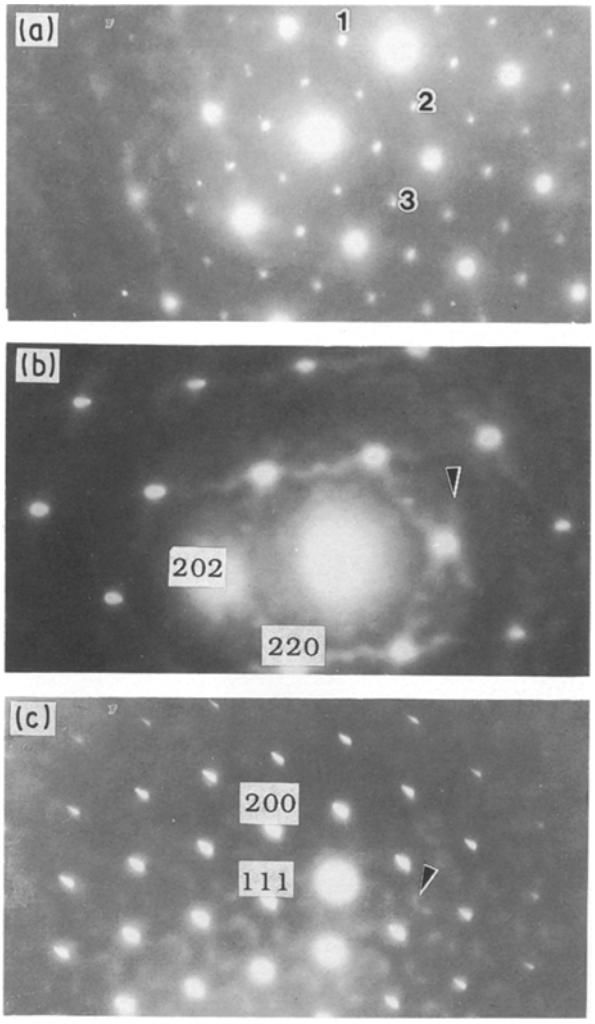

Figure 6 SAD patterns of (Mg,Ti)-PSZ specimen showing (a) t-spots diffracted from three t-variants, $Z = [\bar{1}\,1\,1]$, 9T; also DSI diffracted from c-matrix: (b) 9T, $Z = [\bar{1}\,1\,1]$; (c) 1T, $Z = [0\,\bar{1}\,1]$.

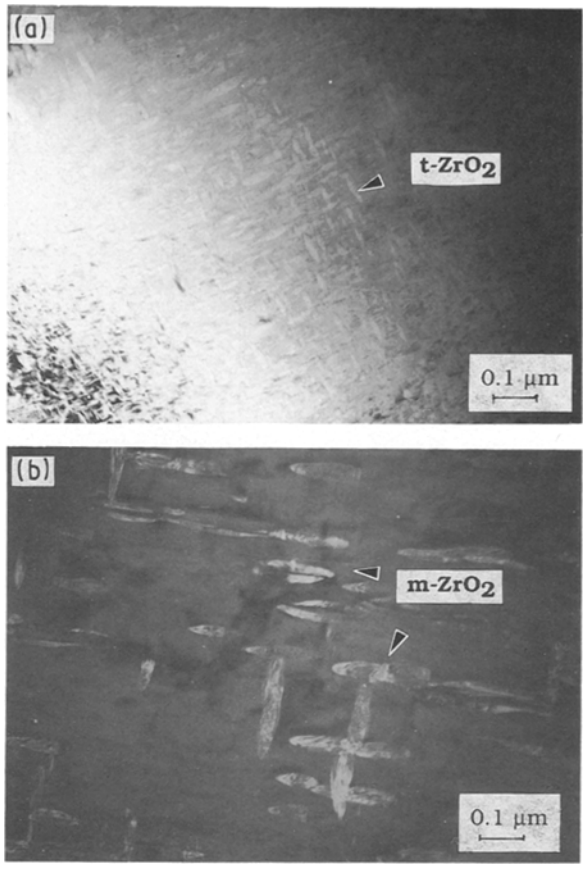

Figure 7 TEM of (Mg,Ti)-PSZ showing (a) bright field image of lenticular t-precipitates in c-matrix of 6T specimen, (b) dark field image ($g = (0\,0\,1)$ spot) of m-phase derived from coarsened t-precipitate in c-matrix of 9T specimen, $Z = [1\,0\,0]$.

TiO_2 content (Fig. 7a and b), but trace analysis indicated that the morphology of the t-phase remained lenticular with a $\{1\,0\,0\}$ habit plane, as in the Mg-PSZ system. The m-phase, formed either by release of matrix constraint at the foil edge or from coarsened t-precipitates in the interior of the (c + t) grain (Fig. 7b), were commonly observed in all the TEM specimens. In addition, m-phase also exists as particles derived probably from t-particles at 1600 °C as discussed below. Note that loop-like features were found in m-phase grains of the 9T specimen (Fig. 8a), but not in 1T (Fig. 8b) and 6T specimens. The (c + t) grains in all the TEM samples were always free of loops. Longitudinal twins and transverse twins of m-phase similar to those found in (Mg,Ti)-PSZ [15] were commonly found in coarsened t-precipitates.

Triple junctions or grain corners of (Mg,Ti)-PSZ do not show evidence of any amorphous phase. Coalescence of zirconia grains may occasionally occur as suggested by the presence of adjacent (c + t)- and m-grains with nearly the same orientation (Fig. 9a). Grain growth of zirconia may also proceed by means of diffusion-induced grain-boundary migration (DIGM) (see Balluffi and Cahn [16] and literature cited therein) as indicated by the corrugated grain boundary (Fig. 9b).

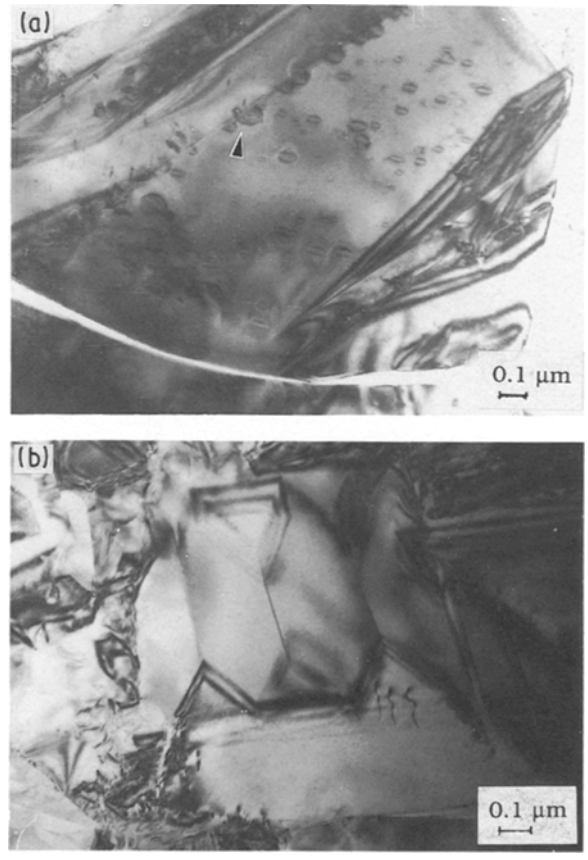

Figure 8 TEM showing (a) loop-like features (arrow) transected by twinning in m-phase of 9T specimen, (b) loop-free m-phase in 1T specimen.

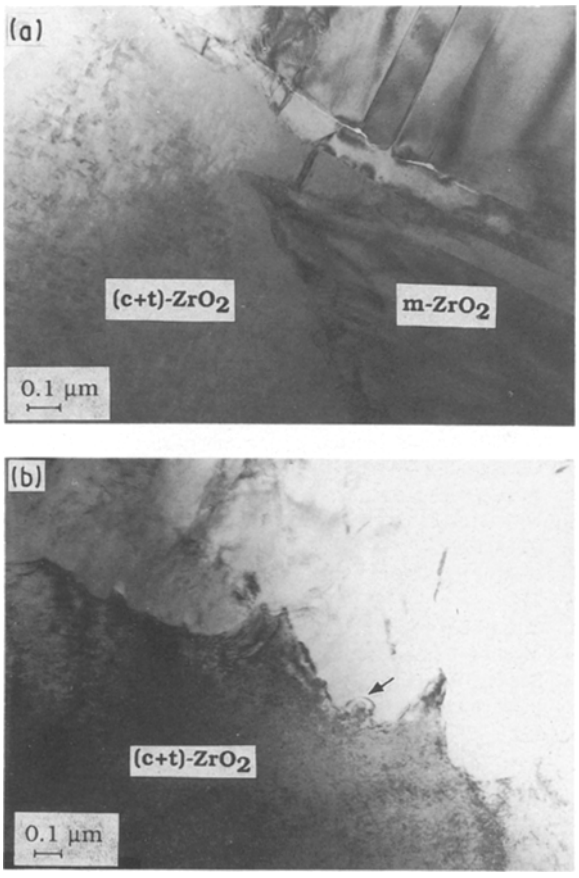

Figure 9 TEM showing (a) coalesced (c + t) and m-grains, $Z = [1\,0\,0]$, 1T; (b) corrugated grain boundary (arrow), 9T specimen.

4. Discussion

4.1. Habit plane and morphology of t-precipitate

In the Mg-PSZ system [6] the habit plane of t-precipitate is predominantly affected by interfacial energy rather than by strain energy because the calculated strain energy is insensitive to orientation deviation from $\{1\,0\,0\}$. The lattice misfit strains ε_{11} and ε_{33} increase with increasing TiO_2 content in (Mg,Ti)-PSZ (Table I). However, the t-ZrO_2 remain lenticular in shape with a $\{1\,0\,0\}$ habit plane as in the Mg-PSZ system. It follows that the morphology and habit plane of t-precipitates in (Mg,Ti)-PSZ should also be affected mainly by interfacial energy. Note that m-variants are longitudinal- and transverse-twinned as in Mg-PSZ [17] and (Mg,Ti)-PSZ systems [15], indicating that m-variants were not modified by the addition of TiO_2.

4.2. Mechanism of microstructural development

Eutectic melting is allowed around 1600 °C for the MgO-TiO_2 pair (eutectic points: 1600 ± 20 °C, MgO with ~ 57 mol % TiO_2; and 1610 ± 20 °C, MgO with ~ 80 mol % TiO_2) [18]. Liquid formation at 1600 °C in the present (Mg,Ti)-PSZ samples was limited as indicated by the shape of the sintered grains (Fig. 5). However, the possibility of the formation of a minor amorphous film at the grain boundary due to trace impurities in the starting powder cannot be ruled out. In general, solid-state sintering and the coalesence of grains (Fig. 9a) are the main mechanisms for microstructural development in the present (Mg,Ti)-PSZ samples. The corrugated grain boundary (Fig. 9b) indicates that chemical inhomogeneity was caused in part by DIGM at 1600 °C.

4.3. Effect of TiO_2 dissolution on t–m transformation

TiO_2 dissolution in ZrO_2 is known to lower the martensitic temperature (M_s) of t–m transformation in pure ZrO_2 [19] and in Y-PSZ [20]. Although the effect of TiO_2 dissolution on M_s in the (Mg,Ti)-PSZ system is not studied, M_s should certainly be lower than the present sintering temperature (1600 °C) according to Coughanour *et al.* [10]. The slight increase of the amount of m-phase with increasing TiO_2 (Fig. 3) must therefore be interpreted as due to the formation of t-phase at the expense of c-phase at 1600 °C and subsequent t–m transformation of the coarsened t-precipitates and particles when the samples were cooled from 1600 °C to room temperature. We have noted the abrupt increase in the amount of the m-phase for specimens containing more than 6 mol % additions of TiO_2. This could be due to an abrupt increase (for whatever reasons) in the number of t-precipitates and particles reaching the critical size for t–m transformation. Alternatively, the presence of $ZrTiO_4$ could cause thermal mismatch and/or poorer matrix constraint which are among the known parameters controlling the nucleation of the martensitic t–m transformation (see Ruhle and Heuer [21] and literature cited therein). This argument is a distinct possibility in view of the anisotropic expansion of orthorhombic $ZrTiO_4$ and the transformation of $ZrTiO_4$ to a baddeleyite (m-ZrO_2) structure under high pressure [22], indicating that the former is more compressible than the latter.

4.4. Loops and DSI

Since X-ray and electron diffraction and FTIR spectra did not detect any decomposition product (e.g. MgO as in the Mg-PSZ system [11]) in the 9T specimen, the loop-like features in the m-phase grain were interpreted as loops due to the condensation of oxygen vacancies in t-ZrO_2 particles. The loops survived the t–m transformation, as indicated by the shearing of loops through m-twins (Fig. 8a). Loops were not found in (c + t)-ZrO_2 grains because the c-matrix can accommodate a significant amount of oxygen vacancies. This is consistent with the observation that the c-bearing grain (but not the m-grain) shows significant DSI, which has been attributed to the existence of an anisotropic defect displacement field (such as the local relaxation of lattice by oxygen vacancies) along the $\langle 1\,1\,1 \rangle$ directions in the real lattice [23].

Loop-like features were found in the m-phase of the 9T specimen but not in 1T and 6T specimens, indicating that the TiO_2 content affects the formation of loops. The dissolution of TiO_2 in the t-zirconia lattice

does not increase the concentration of oxygen vacancies since Zr^{4+} is replaced by Ti^{4+}. However, existing vacancies may possibly condense to form voids or loops in order to accommodate the distortion of the polyhedron when a significant amount of Ti^{4+} was introduced. Loops may form in the t-lattice either at 1600 °C or upon cooling and survive the subsequent t–m transformation. During the δ-Ni_2Al_3 to β-NiAl transformation, voids or loops were also formed accompanied by the replacement of structural vacancies in δ-Ni_2Al_3 by nickel [24].

5. Conclusions

The following conclusions were drawn from X-ray diffraction, infrared spectroscopy and electron microscopy observations of Mg-PSZ (8 mol % MgO) specimens with added TiO_2, sintered at 1600 °C for 6 h:

1. The solubility limit of TiO_2 in the c-phase is reached at a total addition of ca. 6 mol % at or near 1600 °C.
2. The addition of TiO_2 increases the m-ZrO_2 content upon cooling to room temperature.
3. The t-precipitates in the c-matrix remain lenticular with a $\{1\,0\,0\}$ habit plane.

Acknowledgements

Thanks are due to Mr W. H. Deng for preparing the ion-milled samples.

References

1. D. L. PORTER and A. H. HEUER, *J. Amer. Ceram. Soc.* **60** (1977) 183.
2. C. L. LIN, P. SHEN and D. GAN, *J. Mater. Sci. Lett.* **8** (1989) 395.
3. R. H. J. HANNINK, K. A. JOHNSTON, R. T. PASCOE and R. C. GARVIE, in "Advances in Ceramics", Vol. 3, edited by A. H. Heuer and L. W. Hobbs (American Ceramic Society, Columbus, Ohio, 1981) p. 116.
4. V. LANTERI, A. H. HEUER and T. E. MITCHELL, in "Advances in Ceramics", Vol. 12, edited by N. Claussen, M. Ruhle and A. H. Heuer (American Ceramic Society, Columbus, Ohio, 1984) p. 118.
5. L. K. LENZ, MS thesis, Case Western Reserve University, Cleveland, Ohio (1982).
6. V. LANTERI, T. E. MITCHELL and A. H. HEUER, *J. Amer. Ceram. Soc.* **69** (1986) 564.
7. P. T. CHAO and P. SHEN, *Mater. Sci. Eng.* (*A*) **117** (1989) 191.
8. R. R. LEE and A. H. HEUER, *J. Amer. Ceram. Soc.* **70** (1987) 208.
9. A. G. KHACHATURYAN, "Theory of Structural Transformation in Solids" (Wiley, New York, 1983).
10. L. W. COUGHANOUR, R. S. ROTH, S. MARZULLO and F. E. SENNETT, *J. Res. Natl. Bur. Stand.* (*U.S.*) **54**(4) (1955) 191.
11. C. BATEMAN, M. NOTIS and M. HARMER, in Abstracts of 88th Annual Meeting of the American Ceramic Society, Chicago, Il, USA, April 1986.
12. R. D. SHANNON, *Acta Crystallogr.* **A32** (1976) 751.
13. N. T. McDEVITT and W. L. BAUN, *J. Amer. Ceram. Soc.* **47** (1964) 622.
14. C. M. PHILLIPPI and K. S. MAZDIYASNI, *ibid.* **54** (1971) 254.
15. C. BATEMAN, M. NOTIS and C. LYMAN, in 89th Annual Meeting Ceramographic Exhibit of the American Ceramic Society, Pittsburgh, PA, USA, April 1987.
16. R. W. BALLUFFI and J. W. CAHN, *Acta Metall.* **29** (1981) 493.
17. B. C. MUDDLE and R. H. J. HANNINK, *J. Amer. Ceram. Soc.* **69** (1986) 547.
18. F. MASSAZZA and E. SIRCHIA, *Chim. Ind.* (*Milan*) **40** (1958) 378.
19. F. H. BROWN and P. DUWEZ, *J. Amer. Ceram. Soc.* **37** (1954) 132.
20. C. L. LIN, D. GAN and P. SHEN, *Mater. Sci. Eng. A***129** (1990) 147.
21. M. RUHLE and A. H. HEUER, in "Advances in Ceramics", Vol. 12, edited by N. Claussen, M. Ruhle and A. H. Heuer (American Ceramic Society, Columbus, Ohio, 1984) p. 14.
22. R. W. LYNCH and B. MOROSIN, *J. Amer. Ceram. Soc.* **55** (1972) 409.
23. R. CHAIM and D. G. BANDON, in "Advances in Ceramics", Vol. 12, edited by N. Claussen, M. Ruhle and A. H. Heuer (American Ceramic Society, Columbus, Ohio, 1984) p. 86.
24. P. SHEN, D. GAN and S. L. HWANG, *Mater. Sci. Eng. A* **101** (1988) 143.

Received 8 May 1990
and accepted 15 January 1991